⭗·PLOS | ONE

Transcutaneous Application of Carbon Dioxide (CO$_2$) Induces Mitochondrial Apoptosis in Human Malignant Fibrous Histiocytoma *In Vivo*

Yasuo Onishi[1], Teruya Kawamoto[1]*, Takeshi Ueha[2], Kenta Kishimoto[1], Hitomi Hara[1], Naomasa Fukase[1], Mitsunori Toda[1], Risa Harada[1], Masaya Minoda[1], Yoshitada Sakai[3], Masahiko Miwa[1], Masahiro Kurosaka[1], Toshihiro Akisue[1]

1 Department of Orthopaedic Surgery, Kobe University Graduate School of Medicine, Kusunoki-cho, Chuo-ku, Kobe, Japan, 2 NeoChemir Inc., Gokodori, Chuo-ku, Kobe, Hyogo, Japan, 3 Faculty of Health Care Sciences, Himeji Dokkyo University, Kami-Ohno, Himeji, Hyogo, Japan

Abstract

Mitochondria play an essential role in cellular energy metabolism and apoptosis. Previous studies have demonstrated that decreased mitochondrial biogenesis is associated with cancer progression. In mitochondrial biogenesis, peroxisome proliferator-activated receptor gamma coactivator-1 alpha (PGC-1α) regulates the activities of multiple nuclear receptors and transcription factors involved in mitochondrial proliferation. Previously, we showed that overexpression of PGC-1α leads to mitochondrial proliferation and induces apoptosis in human malignant fibrous histiocytoma (MFH) cells *in vitro*. We also demonstrated that transcutaneous application of carbon dioxide (CO$_2$) to rat skeletal muscle induces PGC-1α expression and causes an increase in mitochondrial proliferation. In this study, we utilized a murine model of human MFH to determine the effect of transcutaneous CO$_2$ exposure on PGC-1α expression, mitochondrial proliferation and cellular apoptosis. PGC-1α expression was evaluated by quantitative real-time PCR, while mitochondrial proliferation was assessed by immunofluorescence staining and the relative copy number of mitochondrial DNA (mtDNA) was assessed by real-time PCR. Immunofluorescence staining and DNA fragmentation assays were used to examine mitochondrial apoptosis. We also evaluated the expression of mitochondrial apoptosis related proteins, such as caspases, cytochorome c and Bax, by immunoblot analysis. We show that transcutaneous application of CO$_2$ induces PGC-1α expression, and increases mitochondrial proliferation and apoptosis of tumor cells, significantly reducing tumor volume. Proteins involved in the mitochondrial apoptotic cascade, including caspase 3 and caspase 9, were elevated in CO$_2$ treated tumors compared to control. We also observed an enrichment of cytochrome c in the cytoplasmic fraction and Bax protein in the mitochondrial fraction of CO$_2$ treated tumors, highlighting the involvement of mitochondria in apoptosis. These data indicate that transcutaneous application of CO$_2$ may represent a novel therapeutic tool in the treatment of human MFH.

Introduction

Musculoskeletal malignancies, particularly high-grade sarcomas such as malignant fibrous histiocytoma (MFH), are clinically aggressive and demonstrate high metastatic behavior in various organs. Although many chemotherapeutic protocols are used to treat human sarcomas, current treatment strategies for high-grade sarcomas are ineffective and the prognosis of patients is poor due to local recurrence and metastases [1]. Therefore, new therapeutic strategies against high-grade sarcomas are required.

Mitochondria are cytoplasmic organelles that play an essential role in cellular energy metabolism and programmed cell death [2]. Previous studies have linked decreases in mitochondrial metabolism and/or mitochondrial number to cancer progression [3,4,5]. Mitochondrial proliferation has also been shown to play an important role in cellular apoptosis and may be an integral part of

a cascade of apoptotic events [6]. Peroxisome proliferator-activated receptor gamma coactivator-1 alpha (PGC-1α) is a multi-functional transcriptional coactivator that regulates the activities of multiple nuclear receptors and transcription factors involved in mitochondrial biogenesis [7]. Specifically, PGC-1α transcriptionally regulates the gene encoding mitochondrial transcription factor A (TFAM), which plays an important role in mitochondrial biogenesis [8]. TFAM expression mirrors the fluctuating levels of mitochondrial DNA (mtDNA) in the cell, and mitochondrial synthesis is stimulated by the PGC-1α/TFAM pathway [8]. We have previously shown that mitochondria abundance is significantly decreased in several human sarcomas compared to benign tumors (unpublished data). Furthermore, we demonstrated that PGC-1α overexpression increases mitochondrial proliferation and induces mitochondrial apoptosis in human

MFH cells *in vitro* (unpublished data). These results suggest that regulation of mitochondrial proliferation via modulation of PGC-1α expression, may be utilized as a useful therapeutic tool for the treatment of human musculoskeletal malignancies.

Carbon dioxide (CO$_2$) therapy in the form of a carbonated spa has been historically used in Europe as an effective treatment for cardiac diseases and skin lesions [9,10]. The therapeutic effects of CO$_2$ are caused by an increase in blood flow and microcirculation, nitric oxide-dependent neocapillary formation, and a partial increase in O$_2$ pressure in the local tissue, known as the Bohr effect [9,10,11]. Previously, we demonstrated that our transcutaneous CO$_2$ therapy to rat skeletal muscle induced PGC-1α expression, and led to an increase in mitochondria [12]. These findings suggest that our transcutaneous CO$_2$ therapy can upregulate the mitochondrial biogenesis through an increase of PGC-1α expression in the treated tissue.

Based on our previous studies in skeletal muscle, we hypothesized that transcutaneous application of CO$_2$ may also induce PGC-1α expression and mitochondrial proliferation in tumor tissue, but in this context lead to tumor cell apoptosis. In this study, we use a murine model of human MFH to investigate the effects of transcutaneous application of CO$_2$ on mitochondrial biogenesis and tumor cell apoptosis.

Results

Transcutaneous Application of CO$_2$ Significantly Reduced MFH Cell Growth *in vivo*

To determine the effect of our CO$_2$ treatment on MFH cell growth *in vivo*, we constructed a murine model of human MFH by transplanting the Nara-H cell line into the dorsal subcutaneous area of mice. Transcutaneous application of CO$_2$ reduced tumor volume by 48% in treated mice compared to controls (p<0.01) (Figure 1A and B). No significant difference in body weight was observed between CO$_2$ treated and control groups (Figure 1C). Thus, transcutaneous application of CO$_2$ had an inhibitory effect on MFH tumor growth *in vivo*, with no observable negative side effects.

Transcutaneous Application of CO$_2$ Up-regulated the PGC-1α-TFAM-mitochondria pathway

To investigate the mechanisms underlying the decrease in tumor volume in CO$_2$ treated mice, we examined the expression of PGC-1α and TFAM in tumor tissue using quantitative real-time PCR (qRT-PCR). PGC-1α and TFAM expression was significantly increased in the CO$_2$ group compared to control animals (p<0.05) (Figure 2A and B). Previous studies have shown that mitochondrial synthesis is stimulated by the PGC-1α/TFAM pathway [8]. Thus, we measured the relative levels of mtDNA to nuclear DNA (nDNA) in both CO$_2$ treated and control groups. mtDNA copy number was significantly higher in the tumors from CO$_2$ treated animals compared to controls (p<0.05) (Figure 2C). Consistent with these findings, immunofluorescence staining of mitochondria revealed that mitochondria levels were elevated in the CO$_2$ treated tumors relative to controls (Figure 2D). Staining of normal muscle tissues as a positive control revealed strong staining (Figure S1).

Mitochondrial Apoptosis was Induced by Transcutaneous Application of CO$_2$ Treatment in Human MFH Cells *in vivo*

We performed immunofluorescence staining for DNA breaks to evaluate the effect of CO$_2$ treatment on MFH cell apoptosis *in vivo*.

We observed an increase in cells with apoptotic nuclei in tumors from the CO$_2$ treated group compared to controls (Figure 3A). Flow cytometry revealed that DNA fragmentation, a measure of apoptosis, was increased in CO$_2$ treated tumors compared to controls (Figure 3B). Taken together, these results indicate that CO$_2$ treatment induced apoptosis in human MFH cells *in vivo*.

We also examined the cleavage of caspases and PARP, and evaluated the expression of cytochrome c and Bax in the mitochondrial and cytoplasmic fractions separately to determine the involvement of mitochondria in the observed apoptosis. Immunoblot analyses revealed increased cleavage products of caspase 3 and 9, and PARP in CO$_2$ treated tumors, but not in the control tumors (Figure 3C). Furthermore, we observed decreased expression of cytochrome c in the mitochondrial fraction and increased expression in the cytoplasmic fraction in the CO$_2$ treated group compared to controls. Conversely, Bax protein was increased in the mitochondrial fraction and was decreased in the cytoplasmic fraction (Figure 3D). Positive bands in immunoblot analyses were semiquantified using densitometrical analyses using the Image J program (NIH, USA, http://rsb.info.nih.gov/ij/). Taken together, these results indicated that the anti-tumoral effect of transcutaneous CO$_2$ treatment in a murine model of human MFH may be mediated via mitochondria induced apoptosis.

Transcutaneous Application of CO$_2$ Treatment Increased Intracellular Ca^{2+} in MFH Cells

We finally investigated the mechanism of the induction of the PGC-1α-TFAM-mitochondria pathway by our system in MFH cells. It has been reported that raising intracellular calcium (Ca^{2+}) concentration induces the PGC-1α expression [13,14], and mitochondrial biogenesis [13,14]. Therefore, we examined the effect of our CO$_2$ treatment on the intracellular Ca^{2+} concentration in human MFH cells *in vivo*. We isolated implanted tumors from mice at 0, 6 and 24 hours after our transcutaneous CO$_2$ treatment, and we evaluated the intracellular Ca^{2+} in the tumors. At 0 and 6 hours after treatment, Ca^{2+} concentration in CO$_2$ treated tumors was significantly higher than that in the control tumors (Figure 4). The elevated relative Ca^{2+} concentration of the CO$_2$ treated cells fell in a time-dependent manner after treatment and was equivalent to that of the cells in untreated control tumors within 24 hours (Figure 4). The results indicated that transcutaneous CO$_2$ exposure increased the intracellular Ca^{2+} concentration in human MFH *in vivo*.

Discussion

A number of studies have shown that decreased mtDNA levels are associated with neoplastic transformation and/or tumor progression [15,16], and that mtDNA plays an important role in apoptosis [17]. Higuchi *et al.* investigated the role of mitochondrial respiration in apoptosis signaling in the human myelogenous leukemia cell line, ML-1a. These studies revealed that respiration-deficient clones were resistant to the tumor necrosis factor-induced apoptosis, whereas the clones reconstituted with normal mtDNA were sensitive [18]. We previously demonstrated that both mtDNA levels and PGC-1α expression were significantly decreased in human sarcoma tissues (unpublished data). Our studies showed that apoptosis could be induced by PGC-1α over-expression, which led to an increase in mtDNA number in human MFH cells (unpublished data). These results indicated that loss of PGC-1α expression and the subsequent decrease in mtDNA may render cells resistant to a certain apoptotic pathway.

The relationship between cancer and CO$_2$ is controversial [19,20,21]. It is well established that CO$_2$ alters the functions of
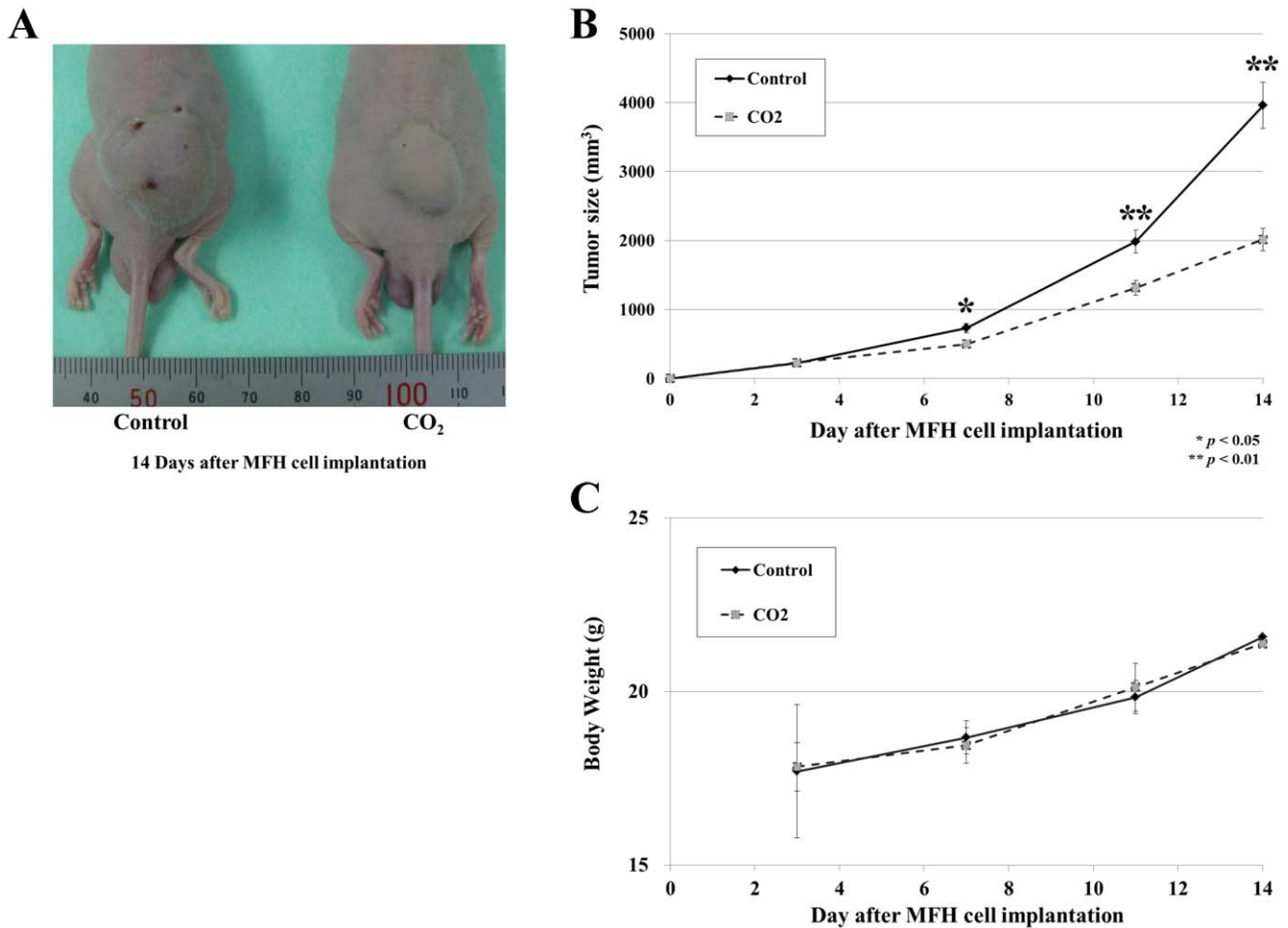
Figure 1. Effect of transcutaneous application of CO₂ on MFH cell growth *in vivo*. Mice were treated with CO₂ or control air three days after MFH cell implantation. Treatment was administered twice weekly for two weeks. (A) MFH tumors in CO₂ treated and control mice, two weeks post-implantation. (B) Tumor volume (mm³) in CO₂ treated or control mice was monitored for two weeks post-implantation. (C) Body weight (g) of CO₂ treated or control mice was monitored for two weeks post-implantation. Data represent the mean $\pm$ S.E of at least three independent experiments (*$p<0.05$, **$p<0.01$).
doi:10.1371/journal.pone.0049189.g001

macrophages and polymorphonuclear cells in the peritoneal and thoracic cavity [22]. While studies exposing tumor cells to CO₂ are not conclusive [23], numerous studies confirm that CO₂ affects the behavior of tumor cells derived from colon carcinomas, adeno-carcinomas and breast cancers [19,20,24]. Although several studies have identified a CO₂-associated increase in tumor cell growth and invasiveness in various cancer cell lines [19,21], there are also reports that show CO₂ can inhibit tumor cells [23,24]. Gutt *et al.* demonstrated that CO₂ increased cell necrosis and decreased proliferation in colonic and pancreatic carcinoma cells [25]. Hao *et al.* reported that exposure of gastric cancer cells to CO₂ pneumoperitoneum significantly induced apoptosis [26]. In the current study, we demonstrate that transcutaneous application of CO₂ to human MFH cells in an engrafted tumor model, upregulated the expression of PGC-1α and TFAM, increased the number of mitochondria, and led to mitochondrial-induced apoptosis. Furthermore, we previously observed a similar effect on human breast cancer cells *in vivo* (Figure S2). Therefore, our transcutaneous CO₂ therapy may have an antitumoral effect on various human malignancies. However, the mechanisms underlying this observation remain unknown. In muscle tissue, mitochondrial respiration is regulated by PGC-1α, which

stimulates various genes associated with mtDNA replication and transcription [7]. Generally, PGC-1α is induced by exercise in muscles, and mediates known responses to exercise such as muscle fiber-type switching and mitochondrial biogenesis [27]. PGC-1α expression is also induced by other stimuli, such as thyroid hormone treatment or 5-aminoimidazole-4-carboxamide-1-β-d-ribofuranoside (AICAR)-induced AMPK activation [28], as well as contractile activity in skeletal muscle [28,29]. Several signaling kinases, after activation of calcium influx, such as p38 [30], AMPK [31] and CaMKIV [32], have also been implicated in mediating transcriptional activation of PGC-1α [33]. We recently demonstrated that transcutaneous application of CO₂ upregulates PGC-1α expression in rat skeletal muscle, establishing a potential link between CO₂ exposure and the induction of mitochondrial biogenesis [12]. It is reported that CO₂ increased the intracellular Ca²⁺ concentration in various cells [34,35], and that the increase in intracellular Ca²⁺ increases the expression of PGC-1α and the amount of mitochondria [13,14,36]. These reports indicated that CO₂ induced the PGC-1α expression and mitochondrial bio-genesis through raising the intracellular Ca²⁺ concentration. In the current study, we have demonstrated that our transcutaneous CO₂ treatment increased the intracellular Ca²⁺ in human MFH cells
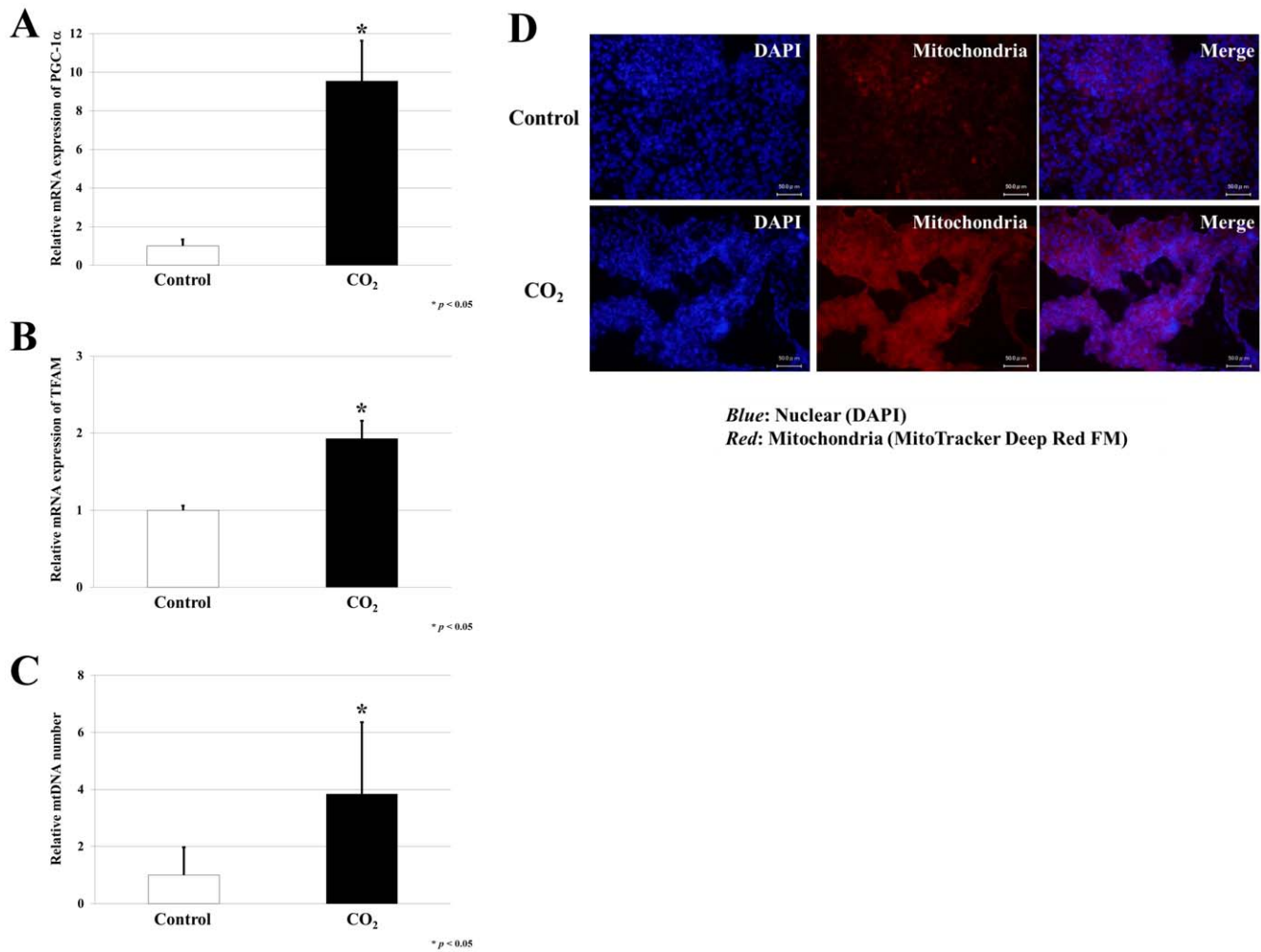
Figure 2. Effect of transcutaneous application of CO$_2$ treatment on mitochondrial proliferation in tumors. qRT-PCR for *PGC-1α* (A) and *TFAM* (B) in CO$_2$ treated or control tumor specimens collected two weeks post-treatment. Expression was normalized to *β-actin* control. Data represent the mean ± S.E of at least three independent experiments (*$p<0.05$). (C) mtDNA was measured in CO$_2$ treated or control tumor samples by PCR and the relative copy number was determined by normalizing to nDNA. Data represent the mean ± S.E. of at least three independent experiments (*$p<0.05$). (D) Immunofluorescence staining of mitochondria in CO$_2$ treated or control tumors after two weeks (*Blue*, nuclear; *Red*, mitochondria).
doi:10.1371/journal.pone.0049189.g002

in vivo. The results strongly support that the effect of our transcutaneous CO$_2$ system on the induction of mitochondrial apoptosis through PGC-1α expression was caused by raising intracellular Ca^{2+} concentration.

We here show that localized, transcutaneous application of CO$_2$ to an *in vivo* model of human MFH led to mitochondria-mediated apoptosis and impaired tumor growth, with no observable effects on body weight, a side effect typically observed following chemotherapy. Although further studies are needed to elucidate the mechanisms of the effects of the treatment on tumor cell apoptosis, our data indicate that transcutaneous application of CO$_2$ may be a useful therapeutic tool for human MFH.

Materials and Methods

Cell Culture

The human MFH cell line, Nara-H (ScienStuff Co., Nara, Japan) [37], was used in this study. Cells were grown in Dulbecco's Modified Eagle's Medium (Sigma-Aldrich Co., St Louis, MO, USA) supplemented with 10% (v/v) fetal bovine serum (Sigma-Aldrich) and 100 U/ml penicillin/streptomycin solution (Sigma-Aldrich). Cells were maintained at 37°C in a humidified 5% CO$_2$ atmosphere.

Animal Models

Male athymic BALB/c nude mice, aged 5–8 weeks were obtained from CLEA Japan, Inc (Tokyo, Japan). Animals were maintained under pathogen-free conditions, in accordance with institutional principles. All animal experiments were performed according to the Guide for the Care and Use of Laboratory Animals at the host institution and were approved by the institutional animal committee (P-101203). Nara-H cells (4.0×10^6 cells in 500 μl PBS) were injected into dorsal, subcutaneous area of mice as previously described [38].

Transcutaneous CO$_2$ Treatment

Transcutaneous application of CO$_2$ was performed as previously described [12]. Briefly, the area of skin around the implanted tumor was treated with CO$_2$ hydrogel. This area was
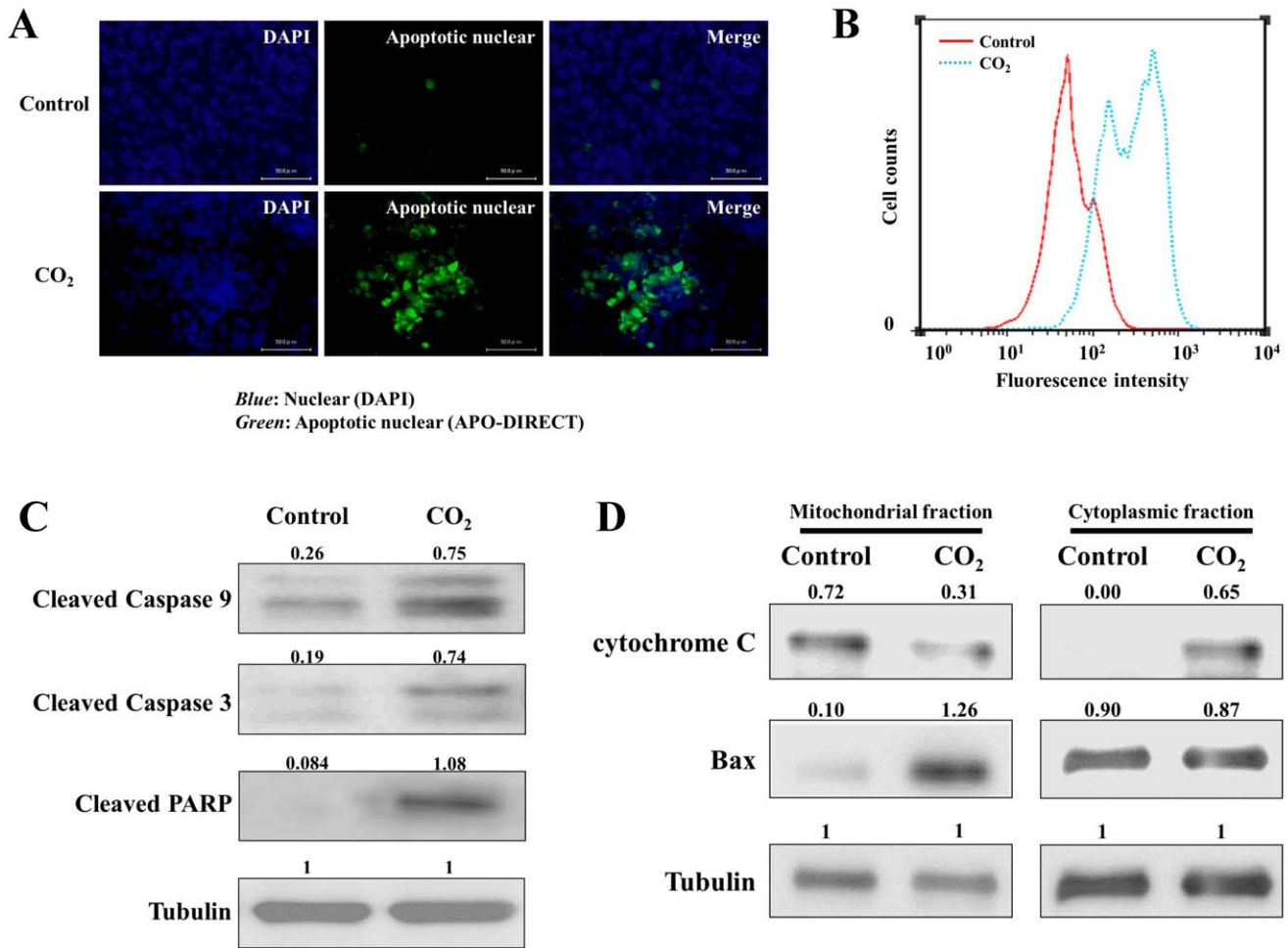
Figure 3. Evaluation of mitochondrial induced apoptosis in CO$_2$ or control treated tumors. (A) DNA fragmentation analysis of tumor samples from CO$_2$ treated and control mice two weeks post-treatment by immunofluorescence. (*Blue*, nuclear; *Green*, apoptosis nuclear) (B) DNA fragmentation was assessed by flow cytometry in CO$_2$ treated tumors (*Blue dots*) and control tumors (*Red*) two weeks post-treatment. (C) Immunoblot analyses determined that increased expression of the cleavage products of caspase 3 and 9, and PARP occurred in the CO$_2$ treated tumors compared to the control tumors. Tubulin was used as an endogenous loading control. (D) Immunoblot analysis of cytochrome c and Bax in mitochondrial and cytoplasmic fractions of CO$_2$ treated and control tumors. Tubulin was used as an endogenous loading control. (C, D) Positive bands in immunoblot analyses were semiquantified using densitometrical analyses using the Image J program (NIH, USA, http://rsb.info.nih.gov/ij/).
doi:10.1371/journal.pone.0049189.g003

then sealed with a polyethylene bag and 100% CO$_2$ gas was administered into the bag (Figure S3). Each treatment was performed for 10 minutes. Control animals were treated similarly, replacing CO$_2$ with an ambient air.

In vivo MFH Tumor Studies

Twenty-four mice were randomly divided into two groups: CO$_2$ group (n = 12) and control group (n = 12). Treatment commenced three days after MFH cell implantation, and was performed twice weekly for 2 weeks. Tumor volume and body weight in mice were monitored twice weekly until the end of the treatment. Tumor volume was calculated as previously described [38] according to the formula $V = \pi/6 \times a^2 \times b$, where a and b represent the shorter and the longer dimensions of the tumor, respectively. At the completion of treatment, all tumors were excised from mice and tissue was stored at -80°C.

Quantitative Real-time PCR

The mRNA expression of PGC-1α and TFAM in implanted tumors was analyzed by quantitative real-time PCR (qRT-PCR)

[39]. Total RNA was extracted from tumor tissues by selective binding to a silica-gel-based membrane using an RNeasy Mini Kit, following the manufacturer's protocol (QIAGEN, Valencia, CA, USA). cDNA was reverse transcribed with 1 μg of total RNA and oligo dT primer by MuLV reverse transcriptase (Applied Biosystems, Foster City, CA, USA). qRT-PCR was performed in a 20 μl reaction using SYBR Green Master Mix reagent (Applied Biosystems) on the ABI prism 7500 sequence detection system (Applied Biosystems). PCR conditions were as follows: 1 cycle at 95°C for 10 minutes followed by 40 cycles at 95°C for 15 seconds and 60°C for 1 minute. Pre-designed primers specific for human *PGC-1α*, human *TFAM* and human *β-actin* were obtained from Invitrogen (Carlsbad, CA, USA). Primer sequences were: PPARGC1A (that encodes PGC-1α), 5′-GGCAGAAGGCAATT-GAAGAG-3′ (forward) and 5′-TCAAAACGGTCCCT-CAGTTC-3′ (reverse); TFAM, 5′-CCGAGGTGGTTTT-CATCTGT-3′ (forward) and 5′-GCATCTGGGTTCTGAGCTTT-3′ (reverse); β-actin, 5′-GAT-CATTGCTCCTCCTGAGC-3′ (forward) and 5′-ACATCTGCTGGAAGGTGGAC-3′ (reverse). The relative ex-
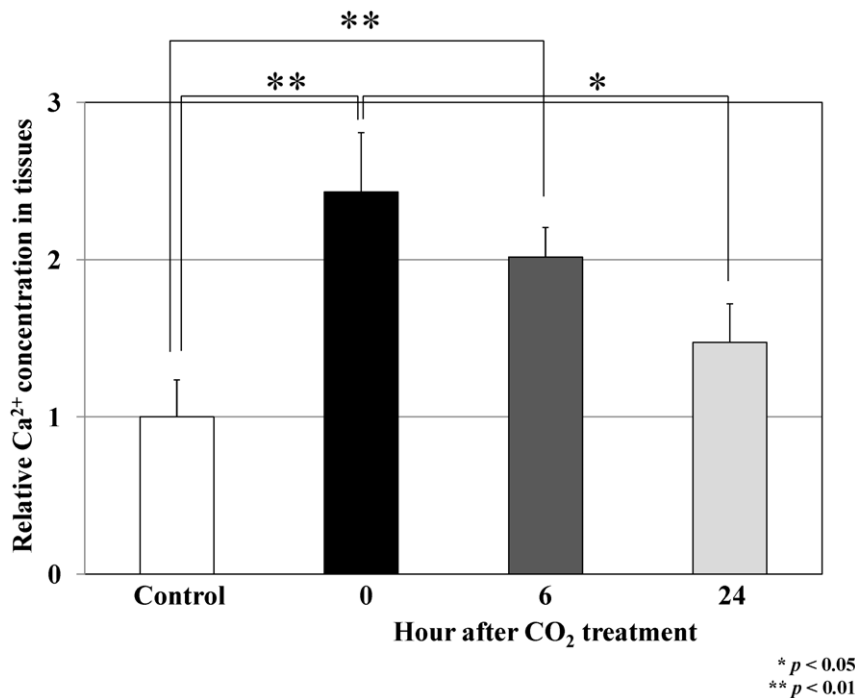
Figure 4. Effect of transcutaneous CO₂ application on intracellular Ca²⁺ concentration in a mouse model of human MFH. Implanted tumors were isolated from mice at 0 (n = 12), 6 (n = 6) and 24 hours (n = 12) after transcutaneous CO₂ exposure, and the intracellular Ca²⁺ concentration was assessed using the Calcium Assay Kit. Data represent the mean ± S.E. of at least three independent experiments (*$p<0.05$, **$p<0.01$).
doi:10.1371/journal.pone.0049189.g004

pression of PGC-1α and TFAM was calculated using the delta-delta Ct method, normalizing to β-actin.

Evaluation of Mitochondrial Proliferation

Mitochondrial proliferation was assessed by determining the relative amount of mtDNA to nuclear (nDNA) in tumor samples. Genomic DNA was isolated from tumor specimens using the GenElute Mammalian Genomic DNA Miniprep Kit (Sigma-Aldrich), and PCR was performed using SYBR Green PCR Master Mix (Applied Biosystems) with primers designed to amplify a region corresponding to nucleotides 16–408 of a D-loop of human mtDNA. The primers used were 5′-GCAGATTTGGG-TACCACCCAAGTATTGACTCACCC-3′ (forward) and 5′-GCATGGAGAGCTCCCGTGAGTGGTTAATAGGGTGA-TAG-3′ (reverse).

Immunofluorescence Staining

To assess the mitochondrial proliferation and the apoptotic activity in treated tumors, we performed the immunofluorescence staining using the MitoTracker Deep Red FM (Invitrogen) and the APO-DIRECT Kit (BD Pharmingen, Franklin Lakes, NJ, USA) following the manufacturer's protocol, respectively. The nucleus was stained with DAPI. The images were obtained using a BZ-8000 confocal microscope (Keyence).

DNA Fragmentation Analysis

DNA fragmentation was evaluated using the APO-DIRECT Kit according to the manufacturer's protocol (BD Pharmingen). Briefly, implanted tumors were excised, minced and filtered through a cell strainer (BD Falcon, Bedford, MA, USA) to obtain a single cell suspension. Erythrocytes were lysed in BD Pharm Lyse™ Lysing Buffer (BD Pharmingen) and the remaining cells

were pelleted and resuspended in PBS. Single cell suspensions were fixed with 1% (v/v) paraformaldehyde and resuspended in 70% (v/v) ice cold ethanol at a concentration of 1×10^6 cells/ml. Each cell pellet was resuspended in 50 μl of DNA Labeling Solution (Reaction Buffer: 10 μl, TdT Enzyme: 0.75 μl, FITC dUTP: 8.0 μl, distilled H₂O: 32.25 μl) and incubated for 60 minutes at 37°C. FITC-dUTP-labeled cells were analyzed by the flow cytometry with a 520 nm Argon laser.

Immunoblot Analysis

Cell lysates were prepared from tumor tissues using a whole cell lysis buffer (Mammalian Protein Extraction Reagent; Thermo Scientific, Rockford, IL, USA) supplemented with protease and phosphatase inhibitors (Roche Applied Science, Indianapolis, IN, USA). Mitochondrial fractions and cytoplasmic fractions were isolated using the Mitochondria Isolation Kit according to manufacturer's protocol (Thermo Scientific), Protein concentration was quantified using the Bradford Protein Assay reagent (Bio-Rad, Richmond, CA, USA) and samples were processed using standard western immunoblotting procedures [39]. Membranes were incubated overnight at 4°C with the following antibodies in Can Get Signal Solution 1 (TOYOBO Co., LTD, Osaka, Japan): anti-human cleaved caspase 3 antibody (1:1000) (Cell Signaling Technology, Danvers, MA, USA), anti-human cleaved caspase 9 antibody (1:1000) (Cell Signaling Technology), anti-human cleaved PARP antibody (1:1000) (Cell Signaling Technology), anti-human cytochrome c antibody (1:1000) (eBiosience Inc., San Diego, CA, USA), anti-human Bax antibody (1:1000) (Cell Signaling Technology) and anti-human α-tubulin antibody (1:2000) (Sigma-Aldrich). Following washes, membranes were incubated with the appropriate secondary antibody conjugated to horseradish peroxidase, and exposed with ECL Plus Western

blotting detection system reagent (GE Healthcare Bio-Sciences, Piscataway, NJ, USA). The signals were detected using the Chemilumino analyzer LAS-3000 mini (Fujifilm, Tokyo, Japan).

Measurement of Intracellular Ca^{2+}

To investigate the effect of transcutaneous CO_2 treatment on intracellular Ca^{2+} in MFH tumor tissues, we isolated implanted tumors from mice at 0 (n = 12), 6 (n = 6) and 24 hours (n = 12) after our transcutaneous CO_2 treatment, and evaluated the intracellular Ca^{2+} concentration using Calcium Assay Kit according to the manufacturer's protocol (Cayman Chemical Company, Ann Arbor, Michigan, USA). Briefly, implanted tumors were excised, minced and rinsed with PBS containing 0.16 mg/ml heparin to remove any extraneous red blood cells and clots, and the tissues were homogenized in PBS containing 0.16 mg/ml heparin. Suspensions were centrifuged at 10000×g for 15 minutes at 4°C, and the supernatant was removed. Then, the detector was added, and the optical density was measured at a wavelength of 570 nm using a Model 680 Microplate Reader (Bio-Rad) after 5 minutes of incubation. The relative number of Ca^{2+} concentration was calculated.

Statistical Analyses

Experiments were performed independently at least three times, and data are presented as the mean ± standard error unless otherwise indicated. Significance of differences between groups was evaluated using a two-tailed Student's *t*-test, and by ANOVA with post hoc test to compare for continuous values. All tests were considered significant at $p < 0.05$.

Supporting Information

Figure S1 Immunofluorescence staining were performed in normal muscle tissues of mice as the control images of staining using the MitoTracker Deep Red FM (Invitrogen). The nucleus was stained with DAPI. The images were obtained using a BZ-8000 confocal microscope (Keyence).
(TIFF)

Figure S2 Effect of our transcutaneous CO_2 treatment on the in vivo tumor growth of human breast cancer cell line, MDA-MB-231. Tumor model mice were created by subcutaneous implantation of the cells (1.5×10^6 cells in 500 μl PBS). Mice were randomly divided into CO_2 group (n = 5) or control group (n = 5), and treatment was performed twice weekly for 15 days. Tumor volume (A) and body weight (B) in mice were monitored until the end of the treatment. (A) At the end of the treatment, we observed a significant decrease in tumor volume in CO_2 group compared with the control group (*p<0.05). (B) No significant difference in body weight was observed between CO_2 treated and control groups.
(TIFF)

Figure S3 Transcutaneous application of CO_2 for a model mouse of human MFH.
(TIFF)

Author Contributions

Conceived and designed the experiments: YO TK TU. Performed the experiments: YO TK TU M. Minoda. Analyzed the data: YO MT RH HH NF. Contributed reagents/materials/analysis tools: TU. Wrote the paper: YO TK TU. Supervised all aspects of this study: KK M. Miwa YS MK TA.

References

1. Le Doussal V, Coindre JM, Leroux A, Hacene K, Terrier P, et al. (1996) Prognostic factors for patients with localized primary malignant fibrous histiocytoma: a multicenter study of 216 patients with multivariate analysis. Cancer 77: 1823–1830.
2. Chen XJ, Butow RA (2005) The organization and inheritance of the mitochondrial genome. Nat Rev Genet 6: 815–825.
3. Verma M, Naviaux RK, Tanaka M, Kumar D, Franceschi C, et al. (2007) Meeting report: mitochondrial DNA and cancer epidemiology. Cancer Res 67: 437–439.
4. Yamada S, Nomoto S, Fujii T, Kaneko T, Takeda S, et al. (2006) Correlation between copy number of mitochondrial DNA and clinico-pathologic parameters of hepatocellular carcinoma. Eur J Surg Oncol 32: 303–307.
5. Yu M, Wan Y, Zou Q (2010) Decreased copy number of mitochondrial DNA in Ewing's sarcoma. Clin Chim Acta 411: 679–683.
6. Kluza J, Marchetti P, Gallego MA, Lancel S, Fournier C, et al. (2004) Mitochondrial proliferation during apoptosis induced by anticancer agents: effects of doxorubicin and mitoxantrone on cancer and cardiac cells. Oncogene 23: 7018–7030.
7. Puigserver P, Spiegelman BM (2003) Peroxisome proliferator-activated receptor-gamma coactivator 1 alpha (PGC-1 alpha): transcriptional coactivator and metabolic regulator. Endocr Rev 24: 78–90.
8. Ekstrand MI, Falkenberg M, Rantanen A, Park CB, Gaspari M, et al. (2004) Mitochondrial transcription factor A regulates mtDNA copy number in mammals. Hum Mol Genet 13: 935–944.
9. Resch KL, Just U (1994) [Possibilities and limits of CO2 balneotherapy]. Wien Med Wochenschr 144: 45–50.
10. Hartmann BR, Bassenge E, Pittler M (1997) Effect of carbon dioxide-enriched water and fresh water on the cutaneous microcirculation and oxygen tension in the skin of the foot. Angiology 48: 337–343.
11. Riggs A (1960) The Nature and Significance of the Bohr Effect in Mammalian Hemoglobins. J Gen Physiol 43: 737–752.
12. Oe K, Ueha T, Sakai Y, Niikura T, Lee SY, et al. (2011) The effect of transcutaneous application of carbon dioxide (CO(2)) on skeletal muscle. Biochem Biophys Res Commun 407: 148–152.
13. Irrcher I, Adhihetty PJ, Sheehan T, Joseph AM, Hood DA (2003) PPARgamma coactivator-1alpha expression during thyroid hormone- and contractile activity-induced mitochondrial adaptations. Am J Physiol Cell Physiol 284: C1669–1677.
14. Ojuka EO, Jones TE, Han DH, Chen M, Holloszy JO (2003) Raising Ca2+ in L6 myotubes mimics effects of exercise on mitochondrial biogenesis in muscle. FASEB J 17: 675–681.
15. Moro L, Arbini AA, Marra E, Greco M (2008) Mitochondrial DNA depletion reduces PARP-1 levels and promotes progression of the neoplastic phenotype in prostate carcinoma. Cell Oncol 30: 307–322.
16. Amuthan G, Biswas G, Zhang SY, Klein-Szanto A, Vijayasarathy C, et al. (2001) Mitochondria-to-nucleus stress signaling induces phenotypic changes, tumor progression and cell invasion. EMBO J 20: 1910–1920.
17. Chandel NS, Schumacker PT (1999) Cells depleted of mitochondrial DNA (rho0) yield insight into physiological mechanisms. FEBS Lett 454: 173–176.
18. Higuchi M, Aggarwal BB, Yeh ET (1997) Activation of CPP32-like protease in tumor necrosis factor-induced apoptosis is dependent on mitochondrial function. J Clin Invest 99: 1751–1758.
19. Jacobi CA, Wenger F, Sabat R, Volk T, Ordemann J, et al. (1998) The impact of laparoscopy with carbon dioxide versus helium on immunologic function and tumor growth in a rat model. Dig Surg 15: 110–116.
20. Lee SW, Southall JC, Allendorf JD, Bessler M, Whelan RL (1999) Tumor proliferative index is higher in mice undergoing laparotomy vs. CO2 pneumoperitoneum. Dis Colon Rectum 42: 477–481.
21. Takiguchi S, Matsuura N, Hamada Y, Taniguchi E, Sekimoto M, et al. (2000) Influence of CO2 pneumoperitoneum during laparoscopic surgery on cancer cell growth. Surg Endosc 14: 41–44.
22. Neuhaus SJ, Watson DI (2004) Pneumoperitoneum and peritoneal surface changes: a review. Surg Endosc 18: 1316–1322.
23. Are C, Talamini MA (2005) Laparoscopy and malignancy. J Laparoendosc Adv Surg Tech A 15: 38–47.
24. Mathew G, Watson DI, Rofe AM, Ellis T, Jamieson GG (1997) Adverse impact of pneumoperitoneum on intraperitoneal implantation and growth of tumour cell suspension in an experimental model. Aust N Z J Surg 67: 289–292.
25. Gutt CN, Bruttel T, Brier C, Paolucci V, Encke A (1998) [CO2 pneumoperitoneum inhibits in vitro proliferation of human carcinoma cells]. Langenbecks Arch Chir Suppl Kongressbd 115: 535–540.

26. Hao YX, Zhong H, Yu PW, Zhang C, Zeng DZ, et al. (2009) Effects of HIF-1alpha on human gastric cancer cell apoptosis at different CO(2) pressures. Clin Exp Med 9: 139–147.
27. Arany Z, Foo SY, Ma Y, Ruas JL, Bommi-Reddy A, et al. (2008) HIF-independent regulation of VEGF and angiogenesis by the transcriptional coactivator PGC-1alpha. Nature 451: 1008–1012.
28. Baar K, Wende AR, Jones TE, Marison M, Nolte LA, et al. (2002) Adaptations of skeletal muscle to exercise: rapid increase in the transcriptional coactivator PGC-1. FASEB J 16: 1879–1886.
29. Pilegaard H, Saltin B, Neufer PD (2003) Exercise induces transient transcriptional activation of the PGC-1alpha gene in human skeletal muscle. J Physiol 546: 851–858.
30. Akimoto T, Sorg BS, Yan Z (2004) Real-time imaging of peroxisome proliferator-activated receptor-gamma coactivator-1alpha promoter activity in skeletal muscles of living mice. Am J Physiol Cell Physiol 287: C790–796.
31. Irrcher I, Ljubicic V, Kirwan AF, Hood DA (2008) AMP-activated protein kinase-regulated activation of the PGC-1alpha promoter in skeletal muscle cells. PLoS One 3: e3614.
32. Wu H, Kanatous SB, Thurmond FA, Gallardo T, Isotani E, et al. (2002) Regulation of mitochondrial biogenesis in skeletal muscle by CaMK. Science 296: 349–352.

33. Lira VA, Benton CR, Yan Z, Bonen A (2010) PGC-1alpha regulation by exercise training and its influences on muscle function and insulin sensitivity. Am J Physiol Endocrinol Metab 299: E145–161.
34. Vadasz I, Dada LA, Briva A, Trejo HE, Welch LC, et al. (2008) AMP-activated protein kinase regulates CO2-induced alveolar epithelial dysfunction in rats and human cells by promoting Na,K-ATPase endocytosis. J Clin Invest 118: 752–762.
35. Summers BA, Overholt JL, Prabhakar NR (2002) CO(2) and pH independently modulate L-type Ca(2+) current in rabbit carotid body glomus cells. J Neurophysiol 88: 604–612.
36. Iwabu M, Yamauchi T, Okada-Iwabu M, Sato K, Nakagawa T, et al. (2010) Adiponectin and AdipoR1 regulate PGC-1alpha and mitochondria by Ca(2+) and AMPK/SIRT1. Nature 464: 1313–1319.
37. Kiyozuka Y, Nakagawa H, Uemura Y, Senzaki H, Yamamoto A, et al. (2001) Novel cell lines established from a human myxoid malignant fibrous histiocytoma arising in the uterus. Cancer Genetics and Cytogenetics 127: 7–15.
38. Okada Y, Akisue T, Hara H, Kishimoto K, Kawamoto T, et al. (2010) The effect of bevacizumab on tumour growth of malignant fibrous histiocytoma in an animal model. Anticancer Res 30: 3391–3395.
39. Takayama K, Ishida K, Matsushita T, Fujita N, Hayashi S, et al. (2009) SIRT1 regulation of apoptosis of human chondrocytes. Arthritis Rheum 60: 2731–2740.